Rev. Adv. Mater. Sci. 37 (2014) 105-110

TENSILE STRENGTH OF GRAPHENE CONTAINING 5-8-5 DEFECTS

A.S. Kochnev[1], I. A. Ovid'ko[1,2,3] and B.N. Semenov[1,2]

[1]Department of Mathematics and Mechanics, St. Petersburg State University, Universitetskii pr. 28, Staryi Peterhof, St. Petersburg 198504, Russia
[2]Institute of Problems of Mechanical Engineering, Russian Academy of Sciences, Bolshoj 61, Vasil. Ostrov, St. Petersburg 199178, Russia
[3]Research Laboratory for Mechanics of New Nanomaterials, St. Petersburg State Polytechnical University, St. Petersburg 195251, Russia

Received: *June 5, 2014*

Abstract. Classical molecular dynamics (MD) with the adaptive intermolecular reactive bond order (AIREBO) potential is used to examine the effect of 5-8-5 defects (divacancies associated with "pentagon-octagon-pentagon" configurations of carbon atoms) on tensile strength of graphene sheets containing such defects. These computer simulations have shown multistage character of fracture processes occurring in graphene sheets containing 5-8-5 defects. In particular, the final stage of fracture is realized through formation of carbon monatomic chains that join separate parts of graphene sheets under mechanical load. Also, it is revealed that the tensile strength significantly degrades (by tens of percent) due to the presence of 5-8-5 defects in graphene.

1. INTRODUCTION

Graphene exhibits superior tensile strength which is important for a wide range of applications; see, e.g., [1-3]. For instance, following the experimental data [1], pristine graphene is characterized by extraordinarily high tensile strength of around 130 GPa. Real graphene sheets/membranes typically contain structural defects strongly influencing their strength and functional properties; see, e.g., reviews [3-6]. So, following experimental data, computer simulations and theoretical examinations, tensile strength of graphene sheets significantly degrades due to the presence of grain boundaries [3,5,7–14]. Also, Stone-Wales defects and vacancies in graphene can decrease its strength; see molecular dynamics simulations [15-17]. At the same time, along with grain boundaries, Stone-Wales defects and vacancies, 5-8-5 defects (divacancies associated with "pentagon-octagon-pentagon" configurations of carbon atoms) can be present in graphene sheets due to irradiation (and other factors) and influence their properties [4,18-23]. In particular, 5-8-5 defects were experimentally observed by transmission electron microscopy in graphene membranes [18,19]. Generally speaking, these defects are capable of strongly affecting both strength and thus lifetime of graphene specimens under mechanical load. In this context, there is large interest in both description of fracture processes in graphene containing 5-8-5 defects and examination of its strength characteristics. The main aims of this paper are to perform computer simulations of the fracture behavior exhibited by graphene containing 5-8-5 defects and reveal their effects on tensile strength of free-standing graphene sheets.

2. SIMULATION METHOD

In description of mechanical loaded sheets of pristine graphene and graphene containing 5-8-5 defects (divacancies associated with "pentagon-octa-

Corresponding author: Ilya Ovid'ko, email: ovidko@nano.ipme.ru

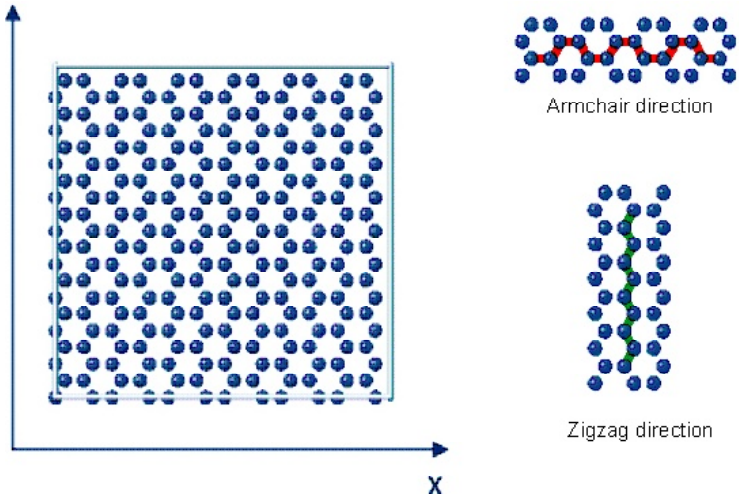

Fig. 1. (Color online) Pristine graphene. The simulation cell with carbon atoms (blue balls) arranged in ideal hexagonal lattice of graphene is shown. The armchair and zigzag directions are oriented along *x* and *y* axes of Cartesian coordinate system.

gon-pentagon" configurations of carbon atoms), we exploited the Large-scale Atomic/Molecular Massively Parallel Simulator (LAMMPS) MD simulation package. In order to specify interatomic bonds, we used the AIREBO potential [24] which is conventionally exploited in computer models of graphene structures. The AIREBO potential is given as follows [24]:

$$E = \frac{1}{2}\sum_{i}\sum_{j\neq i}\left[E_{ij}^{REBO} + E_{ij}^{LJ} + \sum_{k\neq i,j}\sum_{l\neq i,j,k} E_{kijl}^{TORSION}\right]. \quad (1)$$

Here E^{REBO} is the functional form of the Brenner potential for hydrocarbon and carbon systems; E^{LJ} is the slightly modified Lennard-Jones potential, and $E^{TORSION}$ denotes the torsional interaction potential dependent on dihedral angles that specify interatomic interactions in hydrocarbon and carbon systems [20].

In our simulations with the AIREBO potential, the cut-off radius specifying short-range covalent interactions (described by E^{REBO} in formula (1)) is chosen as 2.0 Ångstroms. This value of the cut-off radius is taken, because of its good correspondence to characteristics of real graphene [12].

In order to describe the fracture behavior of graphene sheets, the simulation cells are used with periodic boundary conditions along x and y directions (in the Cartesian coordinate system shown in Fig. 1) The sizes of the simulation cells are chosen as 24.5 nm and 25.5 nm (Fig. 1). The distance between carbon atoms in graphene in its initial (predeformation) state is taken as 1.42 Ångstroms; see review [3] and references therein. In the situation under discussion, the simulation cell contains 240 atoms arranged in 10x12 hexagonal carbon rings (Fig. 1). As it has been demonstrated in Ref. [25], such sizes of the simulation cell are large enough for effective approximate description of the fracture behavior exhibited by graphene. The graphene sheet thickness is taken as 3 Ångstroms.

Before the computer simulation of tensile deformation of graphene, preprocessing was performed to involve NPT simulation (dynamics with constant pressure and constant temperature) during 100 picoseconds at a certain temperature and zero pressure at boundaries of the simulation cell. Then the tensile strain was applied in the *y* direction (in the Cartesian coordinate system shown in Fig. 1a) with a strain rate of 0.05% per picosecond.

3. TENSILE STRENGTH OF PRISTINE GRAPHENE AT ROOM TEMPERATURE

Pristine graphene has a hexagonal crystal lattice with carbon atoms located at lattice nodes (Fig. 1). In this section, we consider fracture processes in pristine graphene under uniaxial tensile load at room temperature (300K). Although computer simulations of the fracture behavior exhibited by pristine graphane under tensile load have been performed earlier (see, e.g., Refs. [25-27]), here we examine pristine graphene as a "reference system" for our further simulations of the fracture behavior of graphene sheets containing 5-8-5 defects (see Section 4). In particular, it is needed for arranging the same simulation procedure for both pristine graphene and graphene containing 5-8-5 defects.

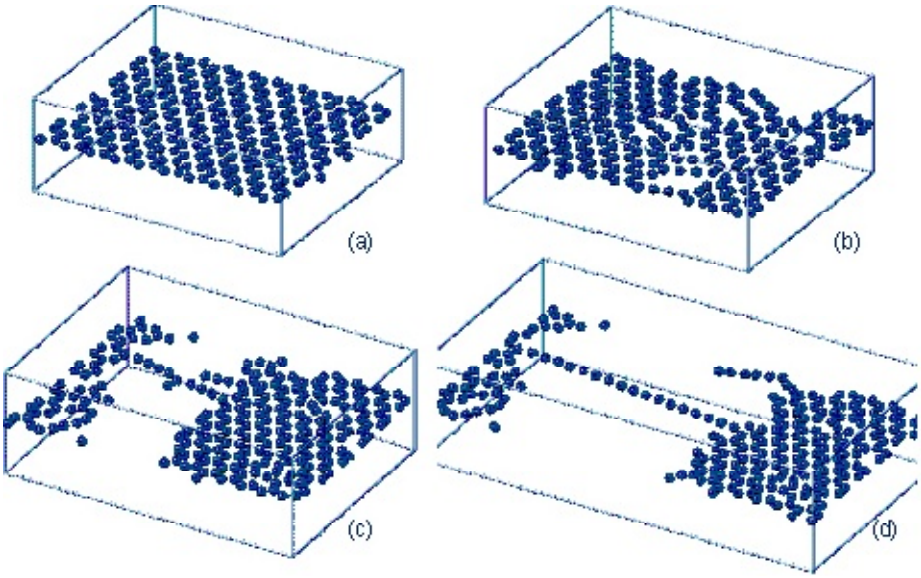

Fig. 2. (Color online) Evolution of pristine graphene under tensile load along the armchair direction of graphene hexagonal lattice (for a detailed description, see the main text).

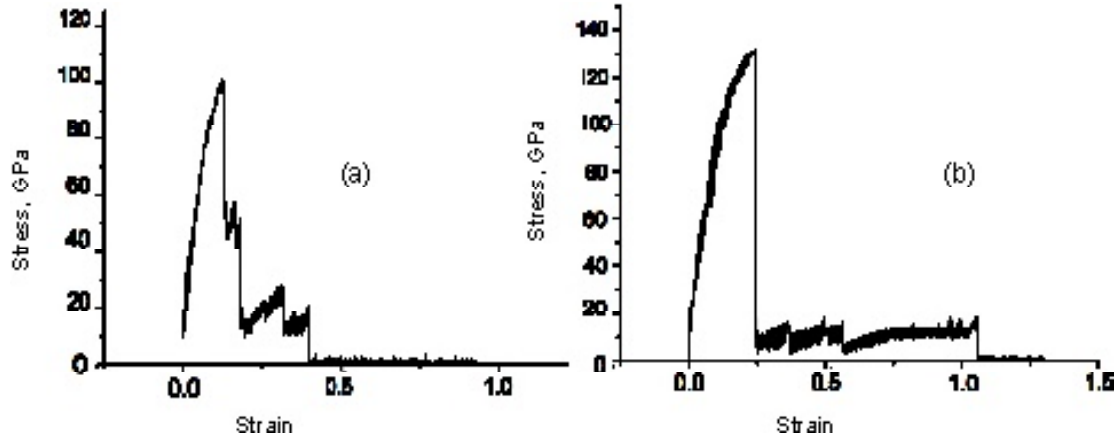

Fig. 3. "Strain-stress" dependences that characterize deformation and fracture processes in pristine graphene deformed along (a) armchair and (b) zigzag crystallographic directions.

In Fig. 2, we present results of our simulations focused on tensile load of pristine graphene along the armchair direction of its hexagonal lattice. As it follows from Fig. 2b, fracture processes are initiated simultaneously in several areas of a pristine graphene sheet. Hexagons of the graphene crystal lattice break in these areas. Also, some carbon atoms are removed from the simulation cell during the fracture processes under discussion. In addition, after separation of a sheet into two parts in the simulation cell, several carbon monatomic chains are formed which join these parts. A similar multistage fracture occurs in the case (which is not illustrated here in simulation figures) of tensile load of pristine graphene along the zigzag direction of its hexagonal lattice.

Figs. 3a and 3b present "strain-stress" dependences that characterize deformation and fracture processes in pristine graphene deformed along the armchair and zigzag crystallographic directions, respectively. These "strain-stress" dependences contain several bursts that reflect the multistage character of the fracture processes. Values of the ultimate tensile strength of a pristine graphene sheet deformed along the armchair and zigzag crystallographic directions are $\sigma_{pr\text{-}armchair}$ = 100 GPa and $\sigma_{pr\text{-}zigzag}$ = 131 GPa, respectively. The second value is well consistent with the experimentally documented [1] value of 130 GPa for graphene.

4. TENSILE STRENGTH OF GRAPHENE SHEETS CONTAINING 5-8-5 DEFECTS AT ROOM TEMPERATURE

Let us present results of computer simulations focused on fracture processes occurring in graphene sheets containing 5-8-5 defects. A typical example

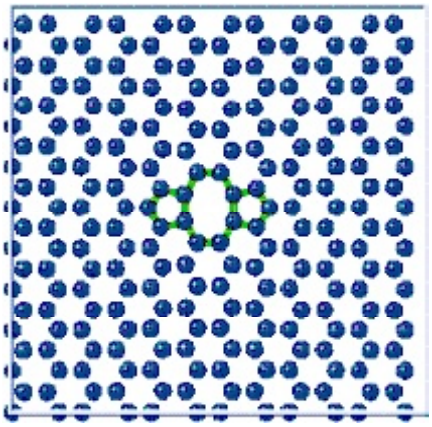

Fig. 4. (Color online) Graphene contains a 5-8-5 defect. The simulation cell with graphene containing a 5-8-5 defect (divacancy associated with "pentagon-octagon-pentagon" configuration of carbon atoms) in its center is shown. "Pentagon-heptagon-pentagon" configuration is arranged along the armchair direction.

of such a defect located in center of the simulation cell is shown in Fig. 4. Following our simulations, evolution of a mechanically loaded graphene sheet containing the 5-8-5 defect (with "pentagon-heptagon-pentagon" configuration being arranged along the armchair direction) is presented in Fig. 5. When the tensile load is applied to the graphene sheet, structural defects carrying fracture – nanoscale voids – are generated in the sheet, first of all, in the vicinity of the 5-8-5 defect (Fig. 5b). With increase in strain degree, nanoscale voids grow and converge, and new nanoscale voids are generated in the sheet (Figs. 5 c and 5d). Then the sheet in the simulation cell breaks into two parts which are joined by a carbon monatomic chain (Fig. 5e). With further increase in strain degree, the length of the monatomic chain significantly grows (Fig. 5f). Finally, the chain breaks, and fracture of the graphene sheet becomes complete.

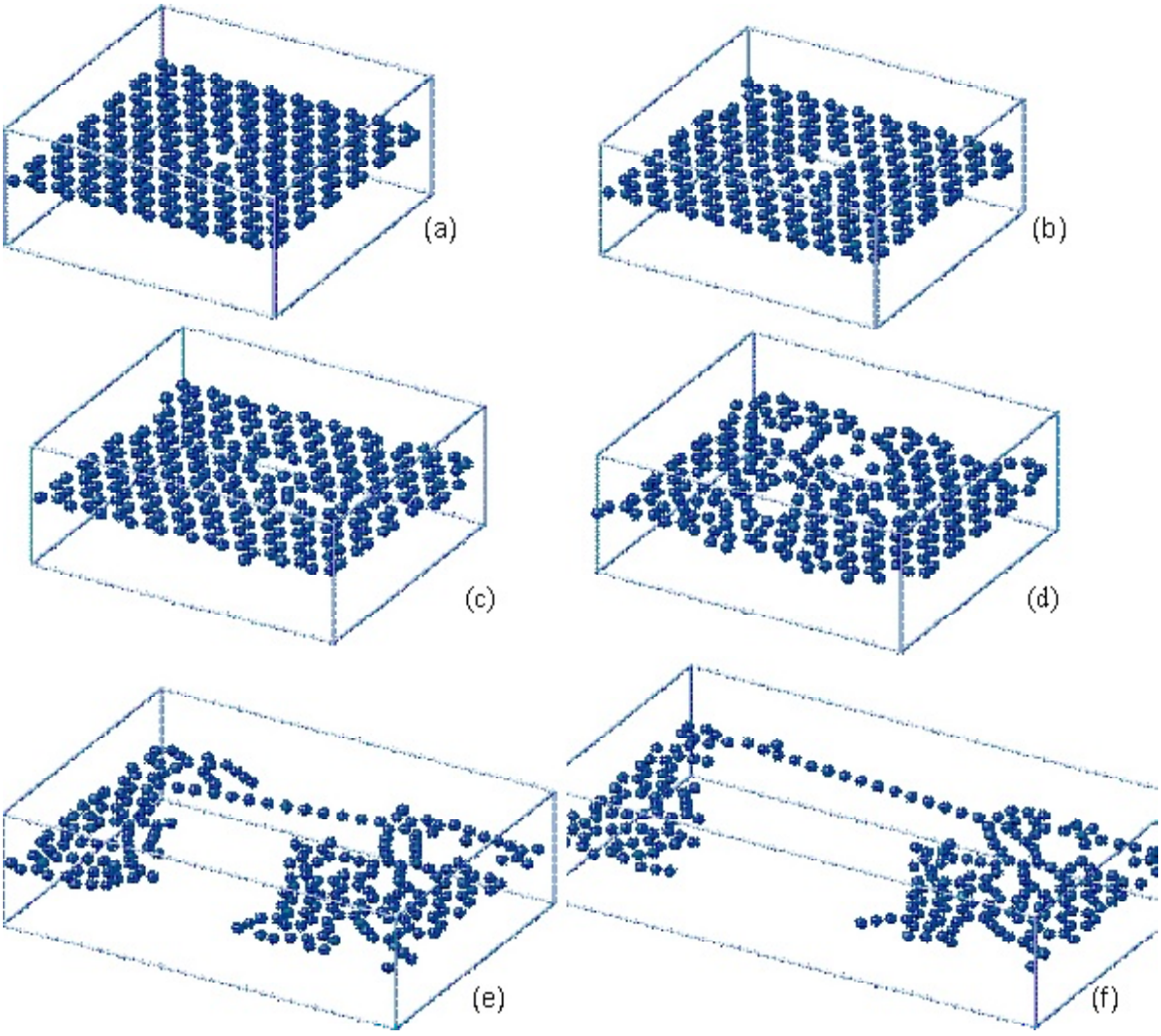

Fig. 5. (Color online) Evolution of graphene sheet with 5-8-5 defect under tensile load along the armchair direction of graphene hexagonal lattice (for a detailed description, see the main text).

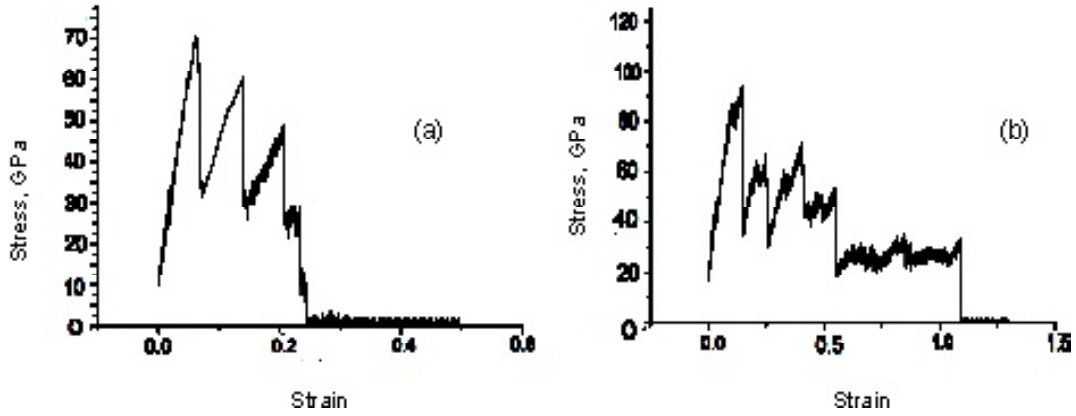

Fig. 6. "Strain-stress" dependences that characterize deformation and fracture processes in graphene with 5-8-5 defect during tensile deformation along (a) armchair and (b) zigzag crystallographic directions.

Figs. 6a and 6b present "strain-stress" dependences that characterize deformation and fracture processes in graphene sheets that contain 5-8-5 defects and are deformed along the armchair and zigzag crystallographic directions, respectively. As with the case of pristine graphene (Fig. 3), these "strain-stress" dependences contain several bursts that reflect the multistage character of the fracture processes in graphene sheets with 5-8-5 defects. Values of the ultimate tensile strength of a graphene sheet with a 5-8-5 defect during its deformation along the armchair and zigzag crystallographic directions are $\sigma_{def\text{-}armchair}$ = 69 GPa and $\sigma_{def\text{-}zigzag}$ = 92 GPa, respectively. These values are significantly lower (by tens of percent), as compared to the corresponding strength values ($\sigma_{pr\text{-}armchair}$ = 100 GPa and $\sigma_{pr\text{-}zigzag}$ = 131 GPa) that specify pristine graphene.

5. CONCLUDING REMARKS

In this paper, we performed MD simulations (with the AIREBO potential) of fracture processes occurring in pristine graphene (serving as a "reference system") and graphene sheets containing 5-8-5 defects. Such defects represent divacancies associated with "pentagon-octagon-pentagon" configurations of carbon atoms in hexagonal crystal lattice of graphene (Fig. 3). The focuses of our research were placed on description of both the specific features inherent to fracture of graphene sheets containing 5-8-5 defects and the effect of these defects on tensile strength of graphene.

The MD simulations have shown multistage character of fracture processes occurring in pristine graphene and graphene sheets containing 5-8-5 defects (see Figs. 2 and 5, respectively). In particular, the final stage of fracture of graphene sheets containing 5-8-5 defects is realized through formation of carbon monatomic chains that join separate parts of the sheets under mechanical load (Figs. 5e and 5f).

Also, with the MD simulations, "strain-stress" dependencies are calculated (Figs. 6 a and 6b) which characterize fracture processes in graphene sheets that contain 5-8-5 defects and are deformed along the armchair and zigzag crystallographic directions, respectively. As with the case of pristine graphene (Fig. 3), these "strain-stress" dependencies contain several bursts that reflect the multistage character of the fracture processes in graphene sheets with 5-8-5 defects. Values of the ultimate tensile strength of a graphene sheet with a 5-8-5 defect during its deformation along the armchair and zigzag crystallographic directions are $\sigma_{def\text{-}armchair}$ = 69 GPa and $\sigma_{def\text{-}zigzag}$ = 92 GPa, respectively. These values are significantly lower (by tens per cent), as compared to the corresponding strength values ($\sigma_{pr\text{-}armchair}$ = 100 GPa and $\sigma_{pr\text{-}zigzag}$ = 131 GPa) that specify pristine graphene. Thus, results of our simulations allow one to conclude that the presence of 5-8-5 defects in graphene sheets leads to a dramatic degradation of tensile strength characterizing these sheets, as compared to tensile strength of their pristine counterparts.

ACKNOWLEDGEMENTS

This work was supported, in part, (for A.S.K. and I.A.O) by the Russian Program "5-100-2020", and (for B.N.S.) by the St. Petersburg State University research grant 6.37.671.2013.

REFERENCES

[1] C. Lee, X. Wei, J.W. Kysar and J. Hone // *Science* **321** (2008) 385.

[2] A.K. Geim // *Science* **324** (2009) 1530.
[3] I.A. Ovid'ko // *Rev. Adv. Mater. Sci.* **34** (2013) 1.
[4] F. Banhart, J. Kotakoski and A.V. Krasheninnikov // *ACS Nano* **5** (2011) 26.
[5] I.A. Ovid'ko // *Rev. Adv. Mater. Sci.* **30** (2012) 201.
[6] L.P. Biro and P. Lambin // *New J. Phys*. **15** (2013) 035024.
[7] P. Y. Huang, C.S. Ruiz-Vargas, A. M. van der Zande, W.S. Whitney, M.P. Levendorf, J.W. Kevek, S. Garg, J.S. Alden, C.J. Hustedt, Y. Zhu, J. Park, P.L. McEuen and D.A. Muller // *Nature* **469** (2011) 389.
[8] C.S. Ruiz-Vargas, H.L. Zhuang, P.Y. Huang, A.M. van der Zande, S. Garg, P.L. McEuen, D.A. Miller, R.C. Hennig and J. Park // *Nano Lett*. **11** (2011) 2259.
[9] R. Grantab, V.B. Shenoy and R.S. Ruoff // *Science* **330** (2010) 946.
[10] Y. Wei, J. Wu, H. Yin, X. Shi, R. Yang and M. Dresselhaus // *Nature Mater*. **11** (2012) 759.
[11] T.-H. Liu, C.-W. Pao and C.-C. Chang // *Carbon* **50** (2012) 3465.
[12] Y.I. Jhon, S.-E. Zhu, J.-H. Ahn and M.S. Jhon // *Carbon* **50** (2012) 3708.
[13] J. Zhang, J. Zhao and J. Lu // *ACS Nano* **6** (2012) 2704.
[14] I.A. Ovid'ko and A.G. Sheinerman // *J. Phys. D: Appl. Phys.* **46** (2013) 345305.
[15] M.C. Wang, C. Yan, L. Ma, N. Hu and M.W. Chen // *Comput. Mater. Sci*. **54** (2012) 236.
[16] J.A. Baimova, L. Bo, S.V. Dmitriev, K. Zhou and A.A. Nazarov // *Europhys. Lett.* **103** (2013) 46001.
[17] C. Carpenter, D. Maroudas and A. Ramasubramaniam // *App. Phys. Lett.* **103** (2013) 013102.
[18] A. Hashimoto, K. Suenaga, A. Gloter, K. Urita and S. Ijima // *Nature* **430** (2004) 870.
[19] M.M. Ugeda, I. Brihuega, F. Hiebel, P. Maller, J.-Y. Veuillen, J.M. Gomez-Rodriguez and F. Yndurain // *Phys. Rev. B*. **85** (2012) 121402 (R).
[20] J. Zhao, H. Zeng and J. Wei // *Physica B* **407** (2012) 204.
[21] Z. Wang, Y.G. Zhou, J. Bang, M.P. Prange, S.B. Zhang and F. Gao // *J. Phys. Chem. C* **116** (2012) 16070.
[22] J.-M. Leyssale and G.L. Vignoles // *J. Phys. Chem. C* **118** (2014) 8200.
[23] O.Ori and M.V. Putz // *Fuller. Nanotubes and Carbon Nanostruct.* **22** (2014) 887.
[24] S.J. Stuart, A.B. Tutein and J.A. Harrison // *J. Chem. Phys.* **112** (2000) 6472.
[25] H. Zhao and N. R. Aluru // *J. Appl. Phys*. **108** (2010) 064321.
[26] T. Shao, B. Wen, R. Melnik, S. Yao, Y. Kawazoe and Y. Tian // *J. Chem. Phys.* **137** (2012) 194901.
[27] F.Liu, P. Ming and J. Li // *Phys. Rev. B* **76** (2007) 064120.